

Absolute Calibration of *Jason-1* and *Envisat* Altimeter Ku-Band Radar Cross Sections from Cross Comparison with TRMM Precipitation Radar Measurements

N. TRAN AND O.-Z. ZANIFE

CLS/Space Oceanography Division, Ramonville St-Agne, France

B. CHAPRON

IFREMER, Brest, France

D. VANDEMARK

NASA GSFC, Wallops Island, Virginia

P. VINCENT

CNES, Toulouse, France

(Manuscript received 1 October 2004, in final form 19 January 2005)

ABSTRACT

One year of collocated, rain-free nadir Ku-band backscatter cross-section measurements from the Tropical Rainfall Mapping Mission (TRMM) precipitation radar (PR) and both *Jason-1* and *Envisat RA-2* altimeter measurements have been compiled to compare these three sources of Ku-band radar cross section. With the exception of a +1.46 dB relative offset between *Jason-1* and PR measurements and a -1.40 dB offset between *Envisat* and PR ones, all three Ku-band measurements compare very well in terms of dependencies upon model wind speed estimates and significant wave height measurements. The altimeter radars and the rain radar thus provide consistent measurements, and observed biases can be rationalized as differences in the radar calibration. The precipitation radar, which also covers off-nadir measurements, has been absolutely calibrated using an active radar calibrator. Consequently, the observed relative offsets can be used to indirectly calibrate both *Jason-1* and *Envisat* altimeter Ku-band radar cross sections in an absolute sense.

1. Introduction

Seven satellite altimeters have been deployed since 1985, providing the first long-term global observations of sea level, wind speed, and wave height. The two latest spacecraft altimeters are *Jason-1* and *Envisat*, launched in December 2001 and March 2002, respectively. Calibration and validation of altimeter data, during dedicated verification phase operations, helped to point out notable differences observed when intercomparing different spaceborne power measurements. The altimeter's normalized radar cross section (so-called σ_0) used to estimate the sea surface wind exhibits platform-

to-platform biases that range from tenths to several decibels (Queffeuilou 2003). Postlaunch absolute radar cross-section calibration has indeed never been performed on past altimeter missions until recently with the launch of the *Envisat RA-2* altimeter. Such an absolute calibration is not essential for the retrieval of altimeter geophysical products. For the σ_0 -derived wind speed product, relative calibration between the different altimeters is sufficient and provides an easy way to make use of previously developed wind speed retrieval algorithms such as the modified Chelton-Wentz (MCW) model (Witter and Chelton 1991) that is based on *Geosat* measurements.

However, the lack of absolute σ_0 calibration for these altimeters does limit the full exploitation of the altimeter measurement information. For example, such calibration would aid efforts related to retrieval of the al-

Corresponding author address: Dr. Ngan Tran, CLS/DOS, 8-10 rue Hermès, 31526 Ramonville St-Agne, France.
E-mail: tran@cls.fr

timetric surface wave period and/or also to extracting quantitative information about short-scale wind wave roughness using both Ku- and C- or S-band data. Absolute calibration is certainly needed to advance theoretical developments on the rough surface scattering, as well as to better combine altimeter measurements with scatterometer and radiometer measurements. Finally, theoretical developments concerning our understanding of the sea state bias would greatly benefit from improved determination of the absolute value of the altimeter radar cross section.

A dedicated field campaign is in progress for the *Envisat* RA-2 altimeter using a ground transponder developed at the European Space Research and Technology Center (ESTEC). The basic absolute calibration requirement for the radar cross-section accuracy is ± 0.2 dB. The results of this campaign are not yet fully available at this time but transponders have been used with success to calibrate other sensors such as the European Remote-Sensing Satellite (ERS) scatterometer (Crapolicchio and Lecomte 1997), designed to measure the near-surface wind field over the oceans. And they are also planned for the future advanced scatterometer (ASCAT) on the meteorological operational (MetOp) platform (Figa-Saldana et al. 2002) in late 2005. Besides such an active calibration, another on-going calibration method for *Envisat* RA-2 uses a passive technique. It is based on the measurement of the receiver noise during a particular mode of operation over well-known natural targets to characterize the receiver in terms of gain and offset (Greco et al. 2001; Pierdicca et al. 2002). In this mode, the altimeter acts like a radiometer. It processes background passive microwave radiation from the earth's surface, corresponding to the receiver thermal noise when no transmitted signal is present; the amount of radiation is then dependent on the nature of the surface viewed at nadir.

Following Freilich and Vanhoff (2003, hereafter FV), our present results use cross comparisons between *Jason-1* and *Envisat* RA-2 with Tropical Rainfall Measuring Mission (TRMM) precipitation radar (PR) measurements. Though designed specifically for the measurements of precipitation profiles in the atmosphere over both land and ocean, the PR system also acquires sea surface backscattering measurements under rain-free conditions. The advantages of using PR data are numerous: 1) it operates at a frequency close to the Ku-band altimeters (13.8 GHz); 2) it provides a high horizontal resolution measurement; 3) the measurements are available in both nadir and near-nadir views; 4) the PR instrument was intensively calibrated and validated through comparisons with an active radar calibrator (ARC) located at a site in Japan, with an

expected absolute accuracy better than 1 dB; and 5) its high vertical resolution helps to filter out rain-contaminated ocean backscatter cross sections.

We compiled 1 yr of collocated data between *Jason-1* and PR and 10 months of collocated data between *Envisat* and PR sensors. Comparisons of both wind speed and wave height dependencies, evaluated through statistical relationships, for the three sources of Ku-band backscatter measurements have been performed, and biases can be determined. This paper contains five sections. Section 2 reviews the need for relative and absolute calibration of altimeter radar backscatter to fulfill specific scientific needs. The three different datasets are presented in section 3 together with collocation criteria and processing procedures. Section 4 compares the wind and wave sensitivities upon the three sources of Ku-band backscatter data. A summary is given in section 5.

2. Relative calibration versus absolute calibration of altimeter radar backscatter

In this section, we review the motivations for both the relative and the absolute calibrations of altimeter backscatter measurements.

a. Relative calibration for operational purpose

The altimeter sea surface wind speed is estimated from backscatter sensitivity to changes in sea surface roughness. The operational wind speed algorithm that is still widely used in altimeter missions (TOPEX/Poseidon, *ERS-1/2*, *Geosat* Follow-On, and *Envisat*) is an early algorithm, by Witter and Chelton (1991), which was developed for *Geosat* data.

This is possible because all altimeters have operated or operate at Ku band. In principle, a wind speed algorithm derived for one altimeter should be directly applicable to another one. Radar cross section is indeed a fundamental property of the sea surface depending on frequency but not on the instrument used to make the measurement. Because of the lack of accurate calibration of the σ_0 against an absolute standard, backscatter estimates are simply adjusted to each other; *Geosat*, as the first mission, is so far the standard reference.

The observed relative Ku-band calibration correction ranges from tenths to several decibels. Statistical cycle monitoring of the σ_0 shows mean values of 11.42, 11.38, and 11.43 dB for TOPEX side A and side B (redundant altimeter turned on) and for TOPEX side B flying on its new orbit (from cycle 365 to cycle 425), respectively. The mean value of *Jason-1* σ_0 measurements is equal to 13.78 dB from geophysical data records (GDRs) over a

period from launch up to cycle 88 (J. Dorandeu 2004, personal communication). Note that these σ_0 values represent the current best understanding of the actual instrument measurement and differ considerably from the TOPEX values with a mean offset of about +2.40 dB in Ku-band (Quartly 2004). The mean value for *Envisat* Ku-band σ_0 is lower at 11.08 dB (cycles 14–26). Note that a bias (−3.24 dB) has been applied on the measurements before their release in the GDR products; removing this bias put the *Envisat* measurement closer to *Jason-1* rather than the TOPEX one within a 1-dB interval.

When computing the wind speed using the MCW model, the TOPEX backscatter σ_0 is offset by −0.63 dB [from comparisons of global histograms of σ_0 with those from *Geosat*, which display an average value of 10.54 dB (Witter and Chelton 1991)]. This model will be referred to as TOPEX MCW and will be used in the following to evaluate offsets.

Developments of new empirical wind model functions still rely on the relative sensitivity of backscatter measurements to wind speed and significant wave height (SWH). These models are derived whether by correlating Ku-band σ_0 with wind speed solely, but through other formalisms (Freilich and Challenor 1994, hereafter FC), or by incorporating extra parameters into the model to take into account the sea state degree of development (Glazman and Greysukh 1993; Lefevre et al. 1994; Gourrion et al. 2002). Such developments only need a consistent relative calibration from one instrument to another one. A relative calibration is also sufficient when further considering the C-band σ_0 (Elfouhaily et al. 1998; Chen et al. 2002).

The *Jason-1* altimeter mission stands out from the others missions by the choice made for the wind speed retrieval. This latter is performed using the model developed by Gourrion et al. (2002) that pointed out evidence that combining Ku-band σ_0 and SWH helps to produce encouraging results with a 10%–15% reduction of rms wind speed error when compared with other existing altimeter wind algorithms. Gommenginger et al. (2002) confirm that this model has the best overall performance compared to TOPEX MCW, Glazman and Greysukh (1993), and FC.

We have not found published results on attempts to derive or apply a dual-parameter algorithm such as the Gourrion et al.’s (2002) using *Envisat* data. To this end, the estimated bias of 2.7 dB between *Jason-1* and *Envisat* radar cross sections from GDR products must be verified to be entirely due to difference in calibration and do not encompass any physical dependencies on wind speed and/or wave height. Hereafter, we shall verify that both *Jason-1* and *Envisat* Ku-band σ_0 mea-

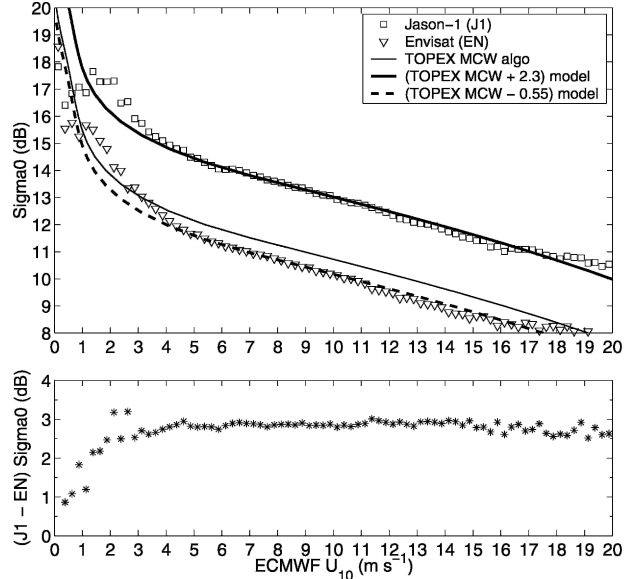


FIG. 1. (top) Binned averages of Ku-band σ_0 measurements from both *Jason-1* and *Envisat* altimeters as a function of sea surface wind. The different curves represent the TOPEX MCW model and offsets from this model of +2.3 and −0.55 dB, at all wind speeds over a 0–20 m s^{-1} interval. (bottom) Difference between *Jason-1* and *Envisat* radar cross sections vs wind speed.

surements exhibit the same wind speed and SWH dependencies.

b. Cross comparison of wind and wave dependencies of Jason-1 and Envisat σ_0

We use independent surface wind speed estimates (U) from the surface model analysis provided by the European Centre for Medium-Range Weather Forecasts (ECMWF) as a common reference to quantify each sensor’s wind dependencies. Sensitivity analysis to SWH uses each respective altimeter’s estimate. Both parameters (ECMWF wind speed estimates and SWH) are available in *Jason-1* and *Envisat* GDR products.

Figure 1 shows the results for the two datasets. For each 1-yr global dataset, the (U , Ku- σ_0) scatter points are binned according to ECMWF wind speed with an interval of 0.1 m s^{-1} , and averaged σ_0 values and standard deviation of the σ_0 are computed for each bin. The data are restricted to latitudes between -65° and $+65^\circ$ in order to compare approximately the same ocean coverage. *Envisat* provides measurements at higher latitudes that are not sampled by *Jason-1* due to the inclination (98.55° versus 66.04°) of its orbit. This selection samples a sufficient range of conditions, allowing display of a clear picture of the wind and SWH effects upon each altimeter’s σ_0 data over a wind speed range from 1 to 20 m s^{-1} . The two statistical relationships

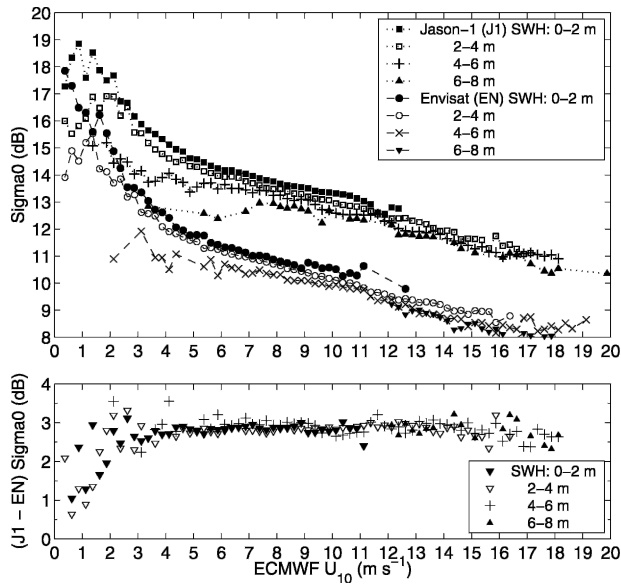


FIG. 2. (top) *Jason-1* and *Envisat* bin-averaged σ_0 as a function of wind speed for four intervals of 2-m SWH values. (bottom) Differences of the above plotted data.

yield the well-known monotonically decreasing function of σ_0 with increasing wind speed. The difference (*Jason-1* minus *Envisat*) of the bin-averaged σ_0 is also given in Fig. 1 (bottom). It displays a nearly constant bias of +2.8 to +3.0 dB for wind speeds between 4 and 15 m s⁻¹. Over this wind speed interval, the wind measurements are heavily populated, providing very low bin-standard deviation estimates. Differences are noisier at low wind speed for three reasons: 1) the highly steep relation between σ_0 and wind, 2) the inherent smoothness associated with the relatively larger spatial and temporal scales of surface wind model estimates, and 3) the lower number of data pairs. The standard TOPEX MCW model is overlaid for comparison with offsets of +2.3 and -0.55 dB, respectively, at all wind speeds. The close correlation of these offset curves with the statistical relationships evaluated respectively for *Jason-1* and *Envisat* confirms that the major difference between altimeter nadir measurements is a constant σ_0 offset over the wind speed interval from 4 to 15 m s⁻¹.

The cross correlation between SWH, σ_0 , and surface wind speed is now addressed. Figure 2 displays the σ_0 bin-averaged relationships versus wind speed for four separate SWH intervals of 2 m (0–2, 2–4, 4–6, and 6–8 m). One observes the clear dependence of altimeter σ_0 upon SWH variation for a given wind speed bin, thanks to the very large amount of data used. This dependency upon SWH is smaller than the dependency upon wind speed. The relative magnitude of the change decreases with increasing wind speed. Over the range of wind

speed, from 4 to 15 m s⁻¹, computations of the differences (*Jason-1* minus *Envisat*) between the four associated statistical relationships exhibit a quasi-constant bias of +2.6 to +3.2 dB. The *Jason-1* and *Envisat* biases are found to be independent of wind speed and SWH over a wind speed range from 4 to 15 m s⁻¹ and for SWH lower than 8. Both Ku-band backscatter measurements present the same wind speed and significant wave height sensitivities.

In the next section, we will provide further calibration information by considering Ku-band backscatter from the TRMM PR instrument. We will perform a similar analysis upon our compilation of two large collocated datasets. The goal is to further assess the respective sensitivity on wind speed and SWH. Before performing this analysis and reporting the findings, we shall first review the expressed needs for accurate absolute calibration and sum up some other benefits that this calibration would bring to altimeter missions.

c. Benefits expected from the absolute calibration of altimeter radar backscatter

Additionally, the continuing effort to improve altimeter-retrieved wind estimates helps to better understand the sensor physics and relationships between the wind, the sea surface roughness, and the altimeter measurements not only in terms of backscatter cross section but also in terms of altimeter range estimates. Indeed, the “sea state bias” correction to the range measurements (e.g., Fu and Glazman 1991) shall certainly benefit from any progress made in this domain. To date, the correction relies on an empirical model that is a function of both wind speed (σ_0 in fact) and wave height (Gaspar and Florens 1998; Gaspar et al. 2002). Despite numerous efforts performed by different teams of experts that concurred to advance our knowledge on how to improve this correction (Gaspar and Florens 1998; Gaspar et al. 2002; Vandemark et al. 2002; Millet et al. 2003a,b; Labroue et al. 2004), refinements on this correction are still necessary and expected. Errors in this estimation actually represent a significant limitation on the accuracy at which global sea level rise can be inferred by altimetry alone (Leuliette et al. 2004).

An absolute calibration of the altimeter radar cross section would represent one step further toward a better understanding of the processes causing electromagnetic scattering from the rough ocean surface. This will in turn help to quantitatively compare data and theoretical models to distinguish between instrumental and physical processes entering the sea state bias correction. This would help to overcome the present limitations that several ongoing studies run into in the understanding of different aspects, namely, the wind-induced

short-scale modulation, the sea state degree of development signatures, the statistical description of the sea surface, and the interaction of electromagnetic radiation with this surface (Elfouhaily et al. 2001; Chapron et al. 2001). Furthermore, future off-nadir altimeter measurements would also directly benefit from this effort.

Results reported by FV represent the first attempt using spaceborne data (from namely the TRMM PR) to quantitatively examine the magnitudes and wind speed dependencies of Ku-band (13.8 GHz) effective nadir reflectivity coefficient and effective mean square slope (mss). The latter represents the two key parameters in the simple geometric optics-scattering formulation relating σ_0 to near-nadir surface roughness and surface dielectric properties (see Brown 1990 for review). The results highlight the potential benefit of accurate absolute calibration of σ_0 to provide more accurate sea surface slope variance from spaceborne σ_0 . This retrieval from the *Seasat*, *Geosat*, and TOPEX did produce values in Ku-band that were unexpectedly higher than the optical measurement of Cox and Munk (1954). From the expected overall sea surface randomness (roughness modulation, local wind fluctuations, etc.), Chapron et al. (2000) considered that the shape of the sea surface slope probability distribution function can partially explain such discrepancies. However, without absolute cross-section measurements, definite conclusions cannot be drawn.

Anderson et al. (2002) also pointed out the limitations they ran into as a result of the lack of absolute calibration of TOPEX σ_0 . They examined the ability of different theoretical models of altimeter backscatter, which combines individual models for air-sea interaction, ocean surface spectrum, and electromagnetic scattering to reproduce and explain observed dependencies on SWH and wave age given by the Gommenginger et al. (2002, hereafter GAL) TOPEX empirical model. As shown in Fig. 4a of their paper, the different Ku-band σ_0 models all reproduce well the qualitative dependence on wind speed but at different σ_0 levels. Also, in Figs. 6b and 7b of their paper, σ_0 estimates exhibit the same behavior with respect to either the wave age or the rms swell height and only differ from each other and from the GAL empirical model by the magnitude of the predicted backscatter. The relative agreement obtained with the different combination of wave spectra and the two descriptions of the interaction between the wind and the sea surface cannot help select the most suitable model. Absolute calibration of the σ_0 would thus clarify the selection of a well-defined description of sea surface, which in turn would provide better insight for the development of semitheoretical models.

Furthermore, the identification of the so-called σ_0 bloom events, which characterize regions exhibiting unusual high σ_0 values, would be facilitated by the determination of a unique threshold to be applied to all altimeters. The bloom events analysis and monitoring would indeed be eased through merging of the different sources of data. The results would be of great interest since the bloom phenomena might be associated with geophysical conditions (other than low wind speeds) such as regions of high productivity as measured by ocean color as suggested by Mitchum et al. (2004). These events represent thus a real physical phenomenon and not just an artifact from a particular system. In particular, Lin et al. (2003) have showed that anomalous backscatter regions observed by the Quick scatterometer (QuikSCAT) often correspond to such phenomena locations as recalled by Mitchum et al. (2004).

Another benefit of the absolute calibration would lie in the better understanding of the ~ 3.5 -dB TOPEX backscattering interfrequency bias observed over ocean (Quarty 2000). It would allow us to quantify which part of it is of physical origin and which part is due to the different calibration of the two frequency bands. Results from absolute calibration are then of prime interest for various investigations. We did not mention developments concerning an altimeter period definition that could certainly favorably use both altimeter frequency measurements (Quilfen et al. 2004). We could also invoke gas exchange studies that can use altimeter frequency differing sensitivity to breaking-wave statistics (Chapron et al. 1995; Elfouhaily et al. 1998; Frew et al. 2001).

3. Data and collocation processing

a. Jason-1 and Envisat altimeter radars

The *Jason-1* altimeter was launched on December 2001 and was placed in the same ground track as its predecessor, TOPEX/Poseidon. This mission is also jointly conducted by the U.S. and French space agencies. It carries the Poseidon-2 altimeter derived from the experimental Poseidon-1 instrument on the TOPEX/Poseidon mission. The satellite flies a non-sun-synchronous orbit at an altitude of 1336 km with an inclination of 66° . Poseidon-2 is a dual-frequency radar altimeter that emits pulses at 13.575 (Ku band) and 5.3 GHz (C band). Detailed descriptions of the mission and the Poseidon-2 instrument are provided by Menard et al. (2003) and Carayon et al. (2003), respectively.

The *Envisat* altimeter (so called RA-2) was launched on March 2002 and is derived from the *ERS-1* and *ERS-2* altimeters (Benveniste et al. 2001). Unlike its predecessors, it is a dual-frequency radar that operates

at Ku band (13.575 GHz) and at S band (3.2 GHz). The satellite orbit is sun-synchronous at an altitude of 800 km with an inclination of 98.55° allowing measurement over the poles. More details can be found in the products handbook (Benveniste et al. 2002).

For this analysis, we used measurements from both *Jason-1* and *Envisat* GDRs over a 1-yr period and a 10-month period (March–December) in 2003, respectively. Although the σ_0 and SWH parameters are provided as 1-s averages in each frequency, here we will only focus on the Ku-band measurements. Interpolated ECMWF surface winds at the measurement location are also provided in the respective products. Any erroneous altimeter estimates are discarded using conventional data quality flagging as recommended by respective user's handbooks (Picot et al. 2003; Benveniste et al. 2002). A further quality check/editing of the data is performed thanks to the Cal/Val products quality assessment routinely performed at Collecte Localisation Satellites (CLS; Dorandeu et al. 2004). We use only rain-free data over ocean surface. Since the *Jason-1* rain flag currently uses a TOPEX-derived algorithm that was not yet fine-tuned on *Jason-1* measurements, we re-computed a *Jason-1* flag by using Tournadre's (2004) algorithm. Among the two *Jason-1* algorithms available, it has been evaluated that Tournadre's algorithm performs better than the Quartly one (Quartly 2004) to detect rain-contaminated data with higher sensitivity to low-intensity rainfall when compared with TRMM Microwave Imager (TMI) rain estimates (Tran et al. 2005).

b. TRMM precipitation radar

In November 1997, the TRMM satellite, a joint U.S. [National Aeronautics and Space Administration (NASA)] and Japan [National Space Development Agency (NASDA)] space agencies project, was successfully launched carrying five instruments including the PR in a non-sun-synchronous orbit. Since the focus of TRMM is to measure rainfall in the Tropics, a low-inclination orbit was selected so that the satellite ground track is confined within 35°S and 35°N. The PR is a Ku-band pulse radar operating at 13.8 GHz that makes backscatter measurements in the atmosphere and from the surface. The sensor antenna is an electronic scanning phased array that scans normal to the flight direction (cross track) through the nadir with measurements at 49 beam positions (e.g., the angle bins 1, 25, and 49 correspond to the incidence angle +18°, 0.1°, and -18°, respectively) over the 215-km swath; the scan duration is equal to 0.6 s with a pixel every 4.3 km both along and across the track (Kozu et al. 2001; Kummerow et al. 1998).

External calibration of the PR, which handles the absolute calibration and monitoring of long-term variations, is performed using an ARC located in Kobe city, Japan. Takahashi et al. (2003) have provided the 4-yr (1998–2001) result of this external calibration experiments. Regarding the transponder mode, among other ones, it shows that the PR has been stable over this time period with fluctuations lower than 0.8 dB.

In August 2001, the TRMM orbit was raised from 350 to 403 km to increase the duration of the mission to 2007. At this higher altitude, the spatial resolution of the PR degraded slightly, the pixel size now being 5.0 km by 5.0 km. The analysis we performed used a 1-yr period over 2003. Over this time frame, there is no published result on the quality of the PR σ_0 (corresponding to the new orbit). Thus we performed a rapid comparison of the PR σ_0 (in the dataset that we are using) with the statistical σ_0 dependence on wind speed derived by FV. This latter was computed by also using 1 yr of data but acquired in the preboost period (August 1999 through July 2000).

We used the TRMM PR standard products, 2A21 in version 5 from the Goddard Distributed Active Archive Center, which include normalized radar cross section measurements along with a rain/no-rain flag for each angle bin (Kummerow et al. 2000) and associated quality flags. For this study, we used only data corresponding to observations at quasi-nadir (0.1° of incidence angle). We discarded all data over land, data with a quality flag set, and rainy ocean data.

Since altimeter σ_0 and SWH are provided in a nominal 1-s averaging period (in fact 1.02 and 1.11 s, respectively for *Jason-1* and *Envisat*) in the altimeter GDR products, we did average the PR σ_0 over two pixels along track to obtain an equivalent \sim 1-s average measurement. This is done before performing the collocations with either *Jason-1* or *Envisat* data. This along-track averaging processing only produces small changes on the PR horizontal resolution (5 km \times 10 km) that remains close to the altimeter one (\sim 6 km \times 7 km).

c. Crossovers selection

The criteria used for the collocation between *Jason-1* (respectively *Envisat*) and PR crossovers are as follows: time separation within 60 min and spatial separation less than 100 km. These large criteria have been set in order to determine how the crossovers are distributed with respect to time lag and distance. This selection resulted in more than 282 000 data points as *Jason-1*/PR crossovers and 154 000 as *Envisat*/PR ones. A subset was then extracted from each collocation dataset to

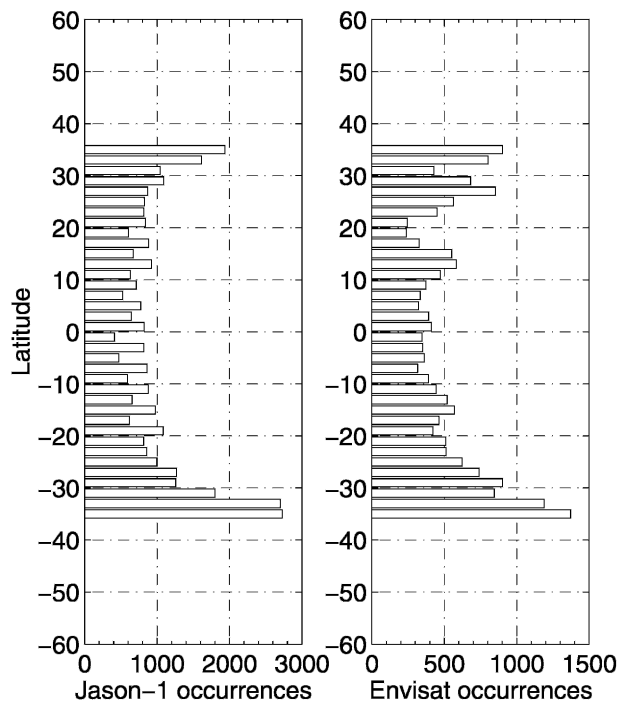


FIG. 3. Histogram of the latitudinal distribution of the crossovers (left) between *Jason-1* and PR and (right) between *Envisat* and PR in the 25-km and 30-min subsets.

keep only crossovers with 30 min and 25 km as time and space separations (approximately 36 000 and 19 800 crossovers left, respectively). The subset allows reasonable comparison of the two independent datasets with high spatial and temporal correlation, large enough data population, and coverage of the entire Tropics. The principle for the pairing of the data between *Jason-1* and PR, for example, is that for each *Jason-1* measurement, we select measurements by PR that match the time window; then among these measurements the closest one is selected if it matches the distance criterion. Otherwise there is no crossover. The collocation set is limited in latitude to the Tropics within $\pm 35^\circ$ of the equator due to TRMM orbits.

Figure 3 shows the latitude distribution of the crossovers for both *Jason-1*/PR and *Envisat*/PR collocation subsets. As can be seen, the density of crossovers is significantly higher at high latitudes than at the equator. This is related to the variation of the orbit track spacing with latitude and the higher revisiting rate at latitudes closer to $\pm 35^\circ$ due to the low inclination of the TRMM orbit. The combination of the different orbit characteristics also leads to a pseudo period of ~ 80 days in the time distribution of crossovers found between *Jason-1* and PR, while the highest occurrences of crossovers are observed at ~ 25 -day intervals in average between *Envisat* and PR in Fig. 4.

4. TRMM PR backscatter versus *Jason-1* and *Envisat* data

To check the quality of the TRMM PR σ_0 in our datasets, we first compare the wind speed dependency of these PR σ_0 with the global TRMM PR model function constructed by FV on preboost PR σ_0 . Freilich and Vanhoff (2003) evaluated this relation using collocations with TMI wind speed estimates. This comparison seems necessary since the absolute calibration published results have been provided for the preboost period when the pixel horizontal resolution was 4.3 km. The postboost measurements that we use here correspond to a slightly degraded resolution (5.0 km).

Again, the ECMWF wind speed estimates from our collocated data subsets have been separated into 0.1 m s^{-1} bins in which the associated σ_0 measurements have been averaged. The bin-averaged relationships derived from the two collocation subsets are plotted in Fig. 5. Also provided are the FV model, the TOPEX MCW model, and the TOPEX MCW model offset by $+0.9 \text{ dB}$ at all wind speed for comparison. As it shows, the averaged relationships and FV model are very close with a slight overestimation by FV over the wind speed range from 3 to $12\text{--}13 \text{ m s}^{-1}$, and differences are larger for lower and higher wind speeds. The steepness of the FV curve is slightly different from the TOPEX MCW model. The FV model is based on an analytic formulation developed by FC that represents the wind speed dependence of σ_0 as the sum of an exponential (important at low wind speeds) and a linear decrease dominant at moderate to high wind speeds. As shown in FV, the best fit to the MCW model function using the FC's formalism is slightly different from the MCW model function itself. While FV showed good matches between the PR data and this FC analytic model, our results show that the MCW slope at moderate wind speeds seems to better reproduce the data behavior as shown with the TOPEX MCW model offset curve. The differences between the PR σ_0 FV's model and the TOPEX MCW model offset curve are in the range of tenths of decibels. So we can conclude that the quality of PR σ_0 from the pre- and the postboost periods, respectively, remains the same. The comparison of the *Jason-1*, *Envisat*, and PR σ_0 should therefore be considered as sufficient and could be used for the absolute calibration of altimeter radar cross sections.

a. Global biases

A first evaluation of the biases between *Jason-1*, *Envisat*, and PR σ_0 has been performed using all 1-yr data sampled between $\pm 35^\circ$ of the equator (not the collo-

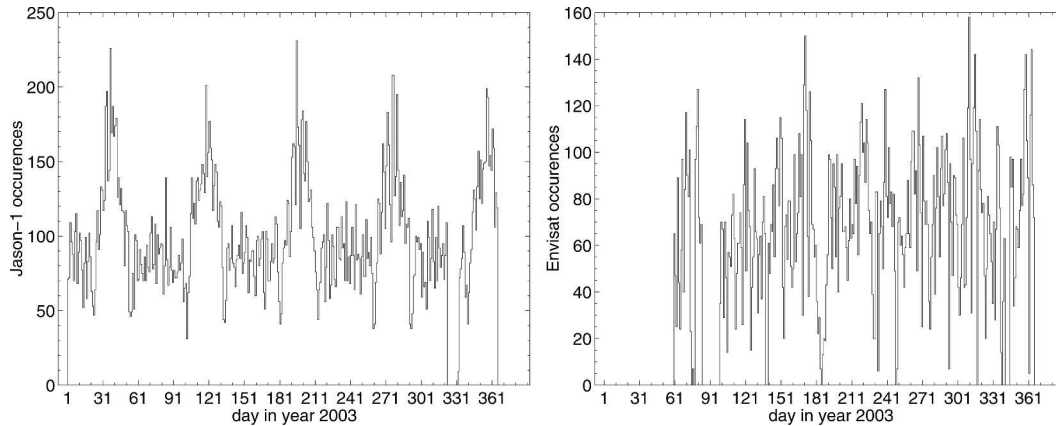


FIG. 4. Histogram of the crossover points (left) between *Jason-1* and PR and (right) between *Envisat* and PR as a function of time in the 100-km and 1-h global sets.

cated sets). Mean values of σ_0 at 12.96, 14.33, and 11.56 dB have been observed, respectively, for the TRMM, *Jason-1*, and *Envisat* radars.

Figure 6 presents histograms of the Ku-band radar cross section from both *Jason-1*/PR and *Envisat*/PR subsets. The data have been binned by intervals of 0.1 dB. The different histograms exhibit similar dissymmetrical shapes with offsets. The *Jason-1* mean value, 14.16 dB, is higher than the PR one at 12.70 dB, while the opposite is observed on the *Envisat*/PR subset. The *Envisat* mean value, 11.34 dB, is lower than the PR one at 12.72 dB. The standard deviations computed from the PR σ_0 distribution showed in both cases larger values, at 1.35 and 1.40 dB, than the altimeter ones that are equal to, respectively, 1.19 and 1.32 dB for *Jason-1* and *Envisat*. As we can see, although the tropical 1-yr datasets and the crossovers subsets do not represent exactly the same geographical distribution of data (and

hence not the same wind speed and significant wave height histograms; not shown), the computed mean values are very close with slightly smaller values for the crossover σ_0 s. The difference is largest between the two evaluations of the PR σ_0 mean, namely 0.25 dB, while it is equal to 0.17 and 0.22 dB, respectively, for *Jason-1* and *Envisat*.

The choice of a 30-min window and 25-km interval allows us to obtain a sufficient number of collocated pairs between the altimeter and the precipitation radar to provide statistically significant results. This large amount of data will be helpful when correlating σ_0 measurements with both wind speed and significant wave height estimates.

To evaluate the stability of the biases, we first computed 10-day averages along the year as shown in Fig. 7, with data from the global collocation sets (100 km; 1-h criteria). The biases are constant over time, and no large drift has been detected by the linear least squares fit (dashed line). The sensitivity of these offsets to the collocation criteria is summarized in Table 1. As one can observe, there is no significant difference either by relaxing the criteria up to 1 h and 100 km or by restricting them down to 5 min and 10 km. The biases are very stable.

We would also like to clarify one of FV's conclusions. Their TRMM PR model function at nadir compared well with *Geosat* results, with an offset of 1.92 dB. The TOPEX altimeter σ_0 being offset by -0.63 dB before using the MCW model, the offset between PR σ_0 s and TOPEX σ_0 s is thus of 1.29 dB. Finally, it must be noted that TRMM PR off-nadir measurements are very consistent with airborne measurements (Jackson et al. 1992; Vandemark et al. 1997). Using a simplified analytical scattering model, FV's reported Ku-band effective reflectivity coefficients are furthermore found to

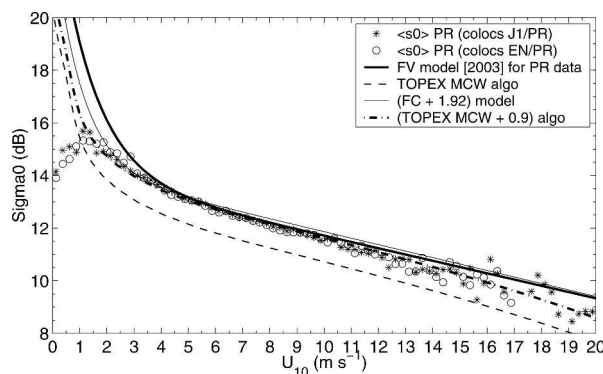


FIG. 5. Bin-averaged PR σ_0 values as a function of surface wind speed from the two yearly collocated subsets. Overlaid are the PR model function derived by FV, the TOPEX MCW model and its curve offset by 0.9 dB, and the FC model function offset by 1.92 dB.

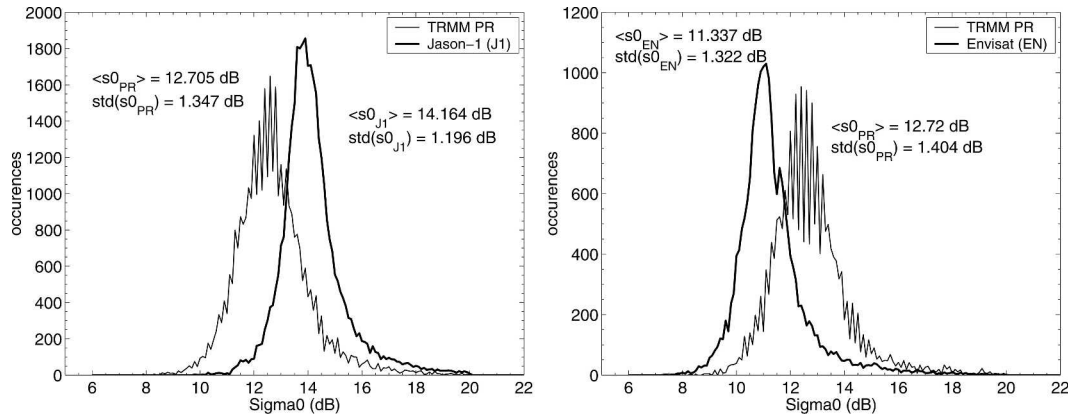


FIG. 6. Histograms of collocated Ku-band σ_0 measurements over the (left) *Jason-1*/PR subset and (right) *Envisat*/PR subset.

closely match theoretical analysis (Jackson et al. 1992; Chapron et al. 2000). The PR σ_0 may thus be reliably considered as absolutely calibrated within 1 dB, in very close agreement with semiempirical efforts that led to an estimate of Ku-band σ_0 of 12.4 dB (± 0.5 dB) at 7 m s^{-1} wind speed (Vandemark et al. 2000).

b. Wind and wave dependencies

Figure 8 presents the PR, *Jason-1*, and *Envisat* bin-averaged relationships correlating σ_0 measurements with wind speed estimates. To assess the representativeness of the tropical collocated datasets, we compare global *Jason-1*- and *Envisat*-derived (all data within $\pm 65^\circ$ of latitudes) statistical relationships and the ones

derived from the collocated subsets. There is no significant difference between the bin-averaged σ_0 estimates from the two types of ocean coverage over the 3–15 m s^{-1} range. The computed statistical relationships are thus meaningful and conclusions based on the collocated data shall be applicable to global data. Overlaid are the curves of the TOPEX MCW model offset by +0.9, +2.3, and -0.55 dB, respectively, to reproduce PR, *Jason-1*, and *Envisat* σ_0 amplitudes and behaviors. We can observe a good match between data and offset curves for wind speed ranging from 4 to 13 m s^{-1} . The σ_0 differences from the bin-averaged data as a function of wind speed (see Fig. 8), show a nearly constant bias of +1.4 to +1.6 dB between *Jason-1* and PR measurements over a wind speed interval from 2 to 12 m s^{-1} . In contrast, we have a negative bias between -1.3 and -1.5 dB for *Envisat*/PR crossovers between 3 and 13 m s^{-1} wind speeds. These two results show that between 3 and 12 m s^{-1} wind speeds, the differences between the altimeter and the rain radar σ_0 are wind speed independent. At lower and higher wind speeds, the bin-averaged estimates have larger error bars, and it is not possible to come to the same conclusion for these less-populated distributions.

We now address the correlation of σ_0 on both wind speed and significant wave height. We will focus on the wind speed values prevailing in the datasets, that is, between 4 and 10 m s^{-1} . In this interval, the dual-dependency of Ku-band σ_0 upon both wind speed and SWH is also pointed out as better defined (Gourrion et al. 2002). Figure 9 illustrates the bin-averaged σ_0 behavior versus wind speed (1 m s^{-1} bin) for four separate intervals of 2-m SWH (0–2, 2–4, 4–6, and 6–8 m) for *Jason-1*, PR, and *Envisat* data from the *Jason-1*/PR and *Envisat*/PR crossovers subsets, respectively. One can observe an obvious dependence of altimeter σ_0 upon

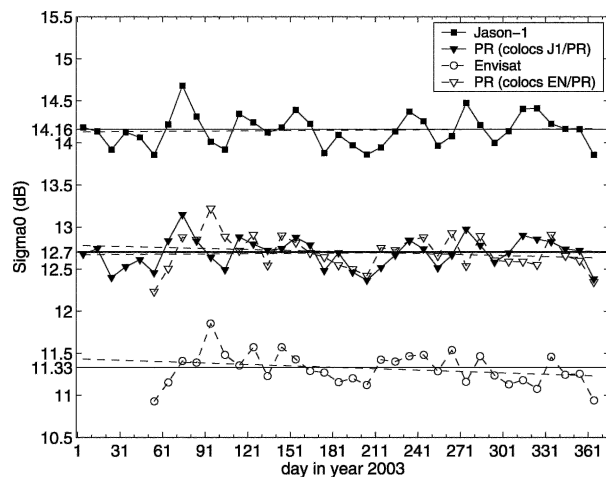


FIG. 7. Evolution of mean σ_0 values computed from the collocated global set as a function of time. Solid curves represent the overall mean σ_0 values for each data source, and dashed lines represent the linear least squares fits to evaluate the stability of the measurements with time.

TABLE 1. Statistical characteristics (mean and std dev) of respectively *Jason-1* and *Envisat*, and PR from the two collocated sets with different filter criteria for time lag and distance between the two radars crossovers

Criteria	N	PR σ_0 (dB)		<i>Jason-1</i> σ_0 (dB)		Criteria	N	PR σ_0 (dB)		<i>Envisat</i> σ_0 (dB)	
		mean	std	mean	std			mean	std	mean	std
100 km and 1 h	282 391	12.70	1.36	14.16	1.18	100 km and 1 h	154 886	12.71	1.41	11.33	1.35
25 km and 30 min	36 058	12.70	1.35	14.16	1.19	25 km and 30 min	19 821	12.72	1.40	11.34	1.32
10 km and 15 min	6714	12.71	1.30	14.16	1.17	10 km and 15 min	3725	12.74	1.44	11.35	1.36
10 km and 5 min	2309	12.68	1.23	14.12	1.09	10 km and 5 min	1195	12.71	1.43	11.32	1.32

SWH variation for a given wind speed. We overlaid second-order polynomial least squares fits. The very large amount of data used to compute the statistical relationships certainly helps this analysis. As altimeter backscatters, the TRMM PR σ_0 exhibits clear dependence on both wind speed and significant wave height. Results of the computation of the bin-averaged σ_0 differences, *Jason-1* minus PR and *Envisat* minus PR, as function of wind speed for the four separate intervals of 2-m SWH are provided in Fig. 10. The differences are nearly constant within 0.15 dB around +1.45 dB for *Jason-1*/PR and within a 0.1-dB interval centered at -1.4 dB for *Envisat*/PR, with no marked trends over the restricted range of wind speed considered. These results lead us to conclude that there is no significant difference between altimeters and precipitation radar

σ_0 measurements in terms of sea surface roughness sensitivity. *Jason-1*, *Envisat*, and PR Ku-band backscatter cross sections respond with a quasi-equivalent sensitivity to both wind speed and significant wave height. We conclude that the relative offsets are due to instrumental calibration biases and do not have a physical origin. Last, note that as expected, the PR σ_0 estimate is less precise than the altimeter ones. Indeed, Fig. 11 shows the standard deviations of the three binned σ_0 s as functions of wind speed and wave height. For wind speeds above 6 m s^{-1} , the TRMM PR σ_0 standard deviation is almost a factor 2 larger than the altimeter σ_0 ones, while this factor decreases down to 1.4–1.6 for lower winds.

5. Summary

Correlations between rain-free Ku-band radar cross sections, measured respectively by *Jason-1* and *Envisat* altimeter radars and TRMM precipitation radar at nadir, with sea surface wind speed and significant wave height estimates, have been analyzed through collocations over a nearly 1-yr-long period. Except for biases, the σ_0 dependence on both wind speed and significant wave height is nearly identical between the three sources of σ_0 measurements. This confirms that the radar cross section is a fundamental property of the sea surface depending on frequency but not on the instrument used to perform the measurement. Table 2 summarizes the different values observed for the offsets through this analysis. The different ways to compute the biases between *Jason-1* and the PR measurements and between *Envisat* and the PR ones provide very similar values. The differences obtained can be attributed to differences in calibration, leading to the conclusion that *Jason-1* data are larger in magnitude by ~ 1.46 dB than the PR ones, while the opposite is observed for *Envisat* measurements, which seem to be lower by ~ 1.40 dB than the PR ones. Note that in the σ_0 values reported in the *Envisat* GDR products, a bias of -3.24 dB has been already applied to make the data consistent with *ERS-2* ones. So removing this constant

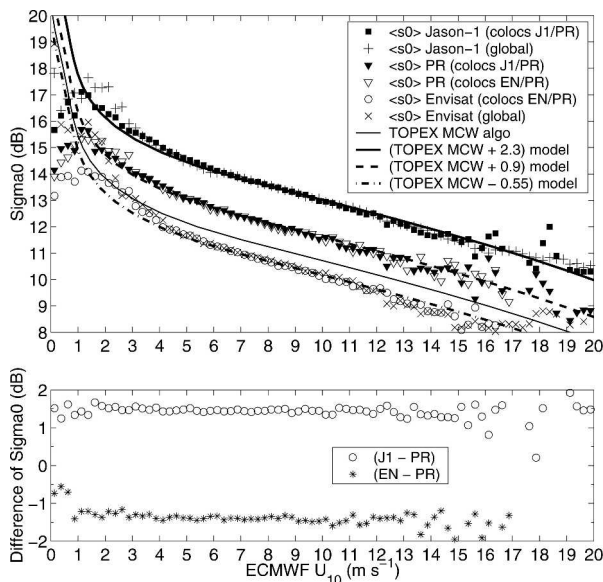


FIG. 8. (top) Binned averages of Ku-band σ_0 measurements from *Jason-1* and *Envisat* altimeters and from TRMM PR as a function of sea surface wind. The different curves represent the TOPEX MCW model and offsets from this model of +2.3, +0.9, and -0.55 dB, at all wind speed over the $0\text{--}20 \text{ m s}^{-1}$ interval. (bottom) Difference between respectively *Jason-1* and *Envisat*, and PR radar cross sections vs wind speed from the collocated subsets.

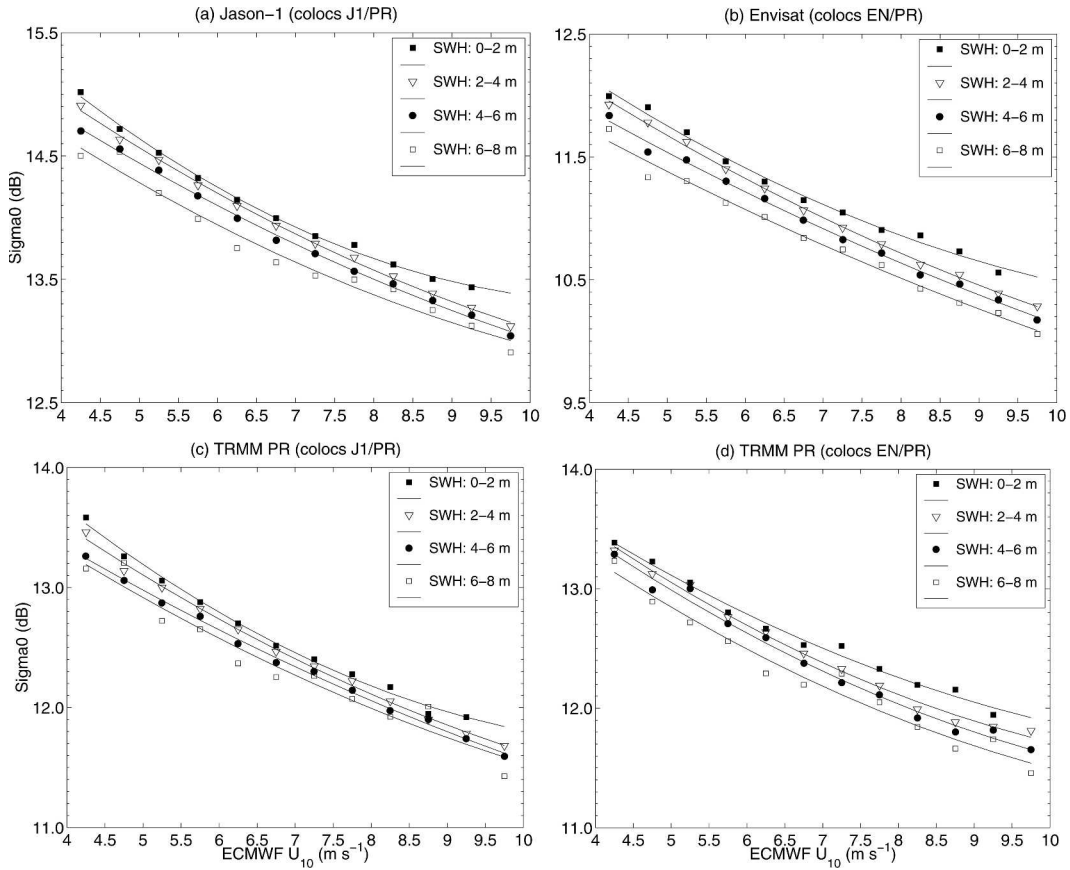


FIG. 9. (a) *Jason-1*, (b) *Envisat*, and (c)–(d) PR bin-averaged σ_0 as a function of wind speed for four intervals of 2-m SWH values from the collocated subsets. The two TRMM PR panels correspond to evaluations over the (c) *Jason-1*/PR and (d) *Envisat*/PR data subsets. Overlaid are second-order polynomial fits to better illustrate the different behaviors.

bias moves *Envisat* values closer to *Jason-1* values, and the relative bias with the PR data becomes +1.84 dB.

Since the on-orbit PR has been absolutely calibrated

using a ground-based active radar calibrator system with accuracy better than 1 dB, these relative biases can be used to calibrate the two *Jason-1* and *Envisat* Ku-band altimeter radars in an absolute way. Further work

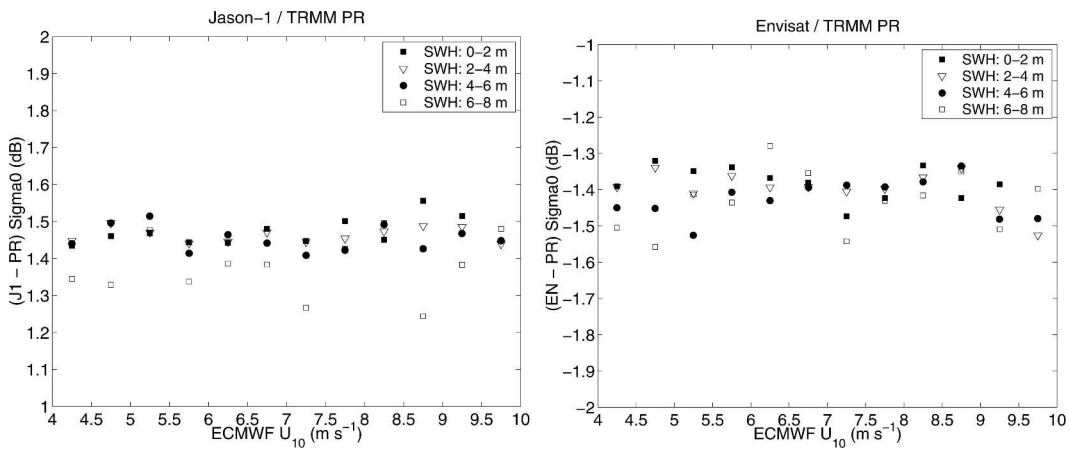


FIG. 10. Differences of the data plotted in Fig. 9.

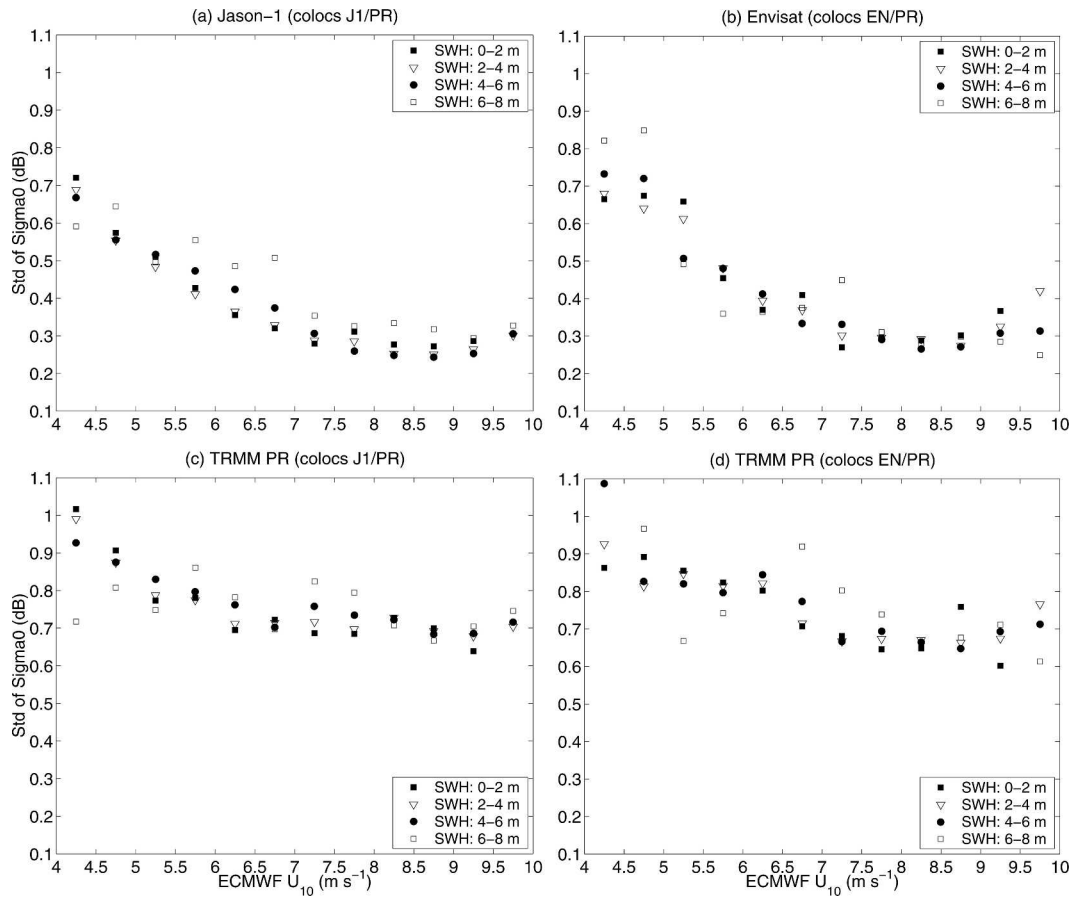


FIG. 11. Standard deviation of binned (a) *Jason-1*, (b) *Envisat*, and (c)–(d) PR σ_0 as a function of wind speed for four intervals of 2-m SWH values from the collocated subsets. The two TRMM PR panels correspond to evaluations over the (c) *Jason-1*/PR and (d) *Envisat*/PR data subsets.

is needed not only to validate the present results (through mostly comparison with the ground transponder measurements performed by ESA for *Envisat RA-2*) but also to characterize the altimeter C-band σ_0 in a similar way.

Two other results came up through this analysis. The offset between TOPEX and PR σ_0 , as observed in this analysis, is ~ 1.29 dB instead of the slightly higher value (1.92 dB) provided by Freilich and Vanhoff (2003). Improved retrieved wind speeds would be obtained for *Envisat* if a two-parameter wind algorithm is consid-

ered upon the present operational model to attenuate the sea state signature on σ_0 . This was advocated earlier by Gourrion et al. (2002), who showed that the TOPEX-generated two-parameter model performed well when applied to *ERS-2* altimeter data after σ_0 constant bias adjustment.

Acknowledgments. We would like to acknowledge the straightforward and rapid electronic access to the TRMM PR data at the Goddard Space Flight Center Distributed Active Archive Center. Thanks are given

TABLE 2. Summary of the different offsets between *Jason-1* and PR, and *Envisat* and PR.

Offset (dB)	Tropics (35°S, 35°N)	Collocations	TOPEX MCW +	Dependency on U	Dependency on (U , SWH)
	mean	mean	σ_0 offset		
	All U values	All U values	U (4–12 m s^{-1})	U (3–13 m s^{-1})	U (4–10 m s^{-1}) SWH (0–6 m)
<i>Jason-1</i> /PR	+1.37	+1.46	+1.4	+1.46	+1.45
<i>Envisat</i> /PR	−1.40	−1.38	−1.45	−1.39	−1.40

to the two anonymous reviewers whose comments helped to improve the clarity of the document. This work was supported by the French space agency (CNES).

REFERENCES

- Anderson, C., J. T. Macklin, C. P. Gommenginger, and M. A. Srokosz, 2002: A comparison of the sea-state sensitivity in empirical and theoretical models of altimeter ocean backscatter. *Can. J. Remote Sens.*, **28**, 475–483.
- Benveniste, J., M. Roca, P. Vincent, G. Levrini, S. Baker, O.-Z. Zanife, and C. Zelli, 2001: The Envisat radar altimetry mission: RA-2, MWR, DORIS and LRR. *ESA Bulletin*, No. 105, ESA Publications, 67–76.
- , and Coauthors, 2002: Envisat RA-2/MWR Product handbook. Doc. PO-TN-ESR-RA-0050. [Available online at http://wwwcpge.mssl.ucl.ac.uk/RA2_Handbook/concepts/ra2/ra2-mwr-PH.html.]
- Brown, G. S., 1990: Quasi-specular scattering from the air-sea interface. *Surface Waves and Fluxes*, W. Plant and G. Geernaerts, Eds., Vol. 2, Kluwer Academic, 1–40.
- Carayon, G., N. Steunou, J.-L. Courriere, and P. Thibaut, 2003: Poseidon-2 radar altimeter design and results of in-flight performances. *Mar. Geod.*, **26**, 156–165.
- Chapron, B., K. Katsaros, T. Elfouhaily, and D. Vandemark, 1995: A note on relationships between sea surface roughness and altimeter backscatter. *Air-Water Gas Transfer*, B. Jähne and E.C. Monahan, Eds., AEON Verlag & Studio, 869–878.
- , V. Kerbaol, D. Vandemark, and T. Elfouhaily, 2000: Importance of peakedness in sea surface slope measurements and applications. *J. Geophys. Res.*, **105**, 17 195–17 202.
- , D. Vandemark, T. Elfouhaily, D. Thomson, P. Gaspar, and S. Labroue, 2001: A new look at global range error estimates. *Geophys. Res. Lett.*, **28**, 3947–3950.
- Chen, G., B. Chapron, R. Ezraty, and D. Vandemark, 2002: A dual-frequency approach for retrieving sea surface wind speed from TOPEX altimetry. *J. Geophys. Res.*, **107**, 3226, doi:10.1029/2001JC001098.
- Cox, C. S., and W. H. Munk, 1954: Measurement of the roughness of the sea surface from photographs of the Sun's glitter. *J. Opt. Soc. Amer.*, **44**, 838–850.
- Crapolicchio, R., and P. Lecomte, 1997: ERS-2 scatterometer calibration and loop performance since launch. *Proc. CEOS Wind and Wave Validation Workshop*, WPP-147, Noordwijk, Netherlands, ESA/ESTEC Publications, ESTEC, 133–144.
- Dorandeu, J., M. Ablain, Y. Faugère, F. Mertz, B. Soussi, and P. Vincent, 2004: Jason-1 global statistical evaluation and performance assessment—Calibration and cross-calibration results. *Mar. Geod.*, **27**, 345–372.
- Elfouhaily, T., D. Vandemark, J. Gourrion, and B. Chapron, 1998: Estimation of wind stress using dual-frequency TOPEX data. *J. Geophys. Res.*, **103**, 25 101–25 108.
- , D. R. Thompson, B. Chapron, and D. Vandemark, 2001: Improved electromagnetic bias theory: Inclusion of hydrodynamic modulations. *J. Geophys. Res.*, **106**, 4655–4663.
- Figa-Saldana, J., J. J. W. Wilson, E. Attema, R. Gelsthorpe, M. R. Drinkwater, and A. Stoffelen, 2002: The advanced scatterometer (ASCAT) on the meteorological operational (MetOp) platform—A follow on the for European wind scatterometers. *Can. J. Remote Sens.*, **28**, 404–412.
- Freilich, M. H., and P. Challenor, 1994: A new approach for determining fully empirical altimeter wind speed model functions. *J. Geophys. Res.*, **99**, 25 051–25 062.
- , and B. A. Vanhoff, 2003: The relationship between winds, surface roughness, and radar backscatter at low incidence angles from TRMM precipitation radar measurements. *J. Atmos. Oceanic Technol.*, **20**, 549–562.
- Frew, N. M., D. M. Glover, and E. J. Bock, 2001: Estimation of air-sea gas transfer using Jason-1 dual-frequency normalized backscatter. *AVISO Newsletter*, No. 8, CNES, 52–53.
- Fu, L. L., and R. Glazman, 1991: The effect of the degree of wave development on the sea state bias in radar altimetry measurements. *J. Geophys. Res.*, **96**, 829–834.
- Gaspar, P., and J.-P. Florens, 1998: Estimation of the sea state bias in radar altimeter measurements of sea level: Results from a new non parametric method. *J. Geophys. Res.*, **103**, 15 803–15 814.
- , S. Labroue, F. Ogor, G. Lafitte, L. Marchal, and M. Rafanel, 2002: Improving nonparametric estimates of the sea state bias in radar altimeter measurements of sea level. *J. Atmos. Oceanic Technol.*, **19**, 1690–1707.
- Glazman, R., and A. Greysukh, 1993: Satellite altimeter measurements of surface wind. *J. Geophys. Res.*, **98**, 2475–2483.
- Gommenginger, C. P., M. A. Srokosz, P. G. Challenor, and P. D. Cotton, 2002: Development and validation of altimeter wind speed algorithms using an extended collocated buoy/TOPEX data set. *IEEE Trans. Geosci. Remote Sens.*, **40**, 251–260.
- Gourrion, J., D. Vandemark, S. Bailey, B. Chapron, C. P. Gommenginger, P. G. Challenor, and M. A. Srokosz, 2002: A two-parameter wind speed algorithm for Ku-band altimeters. *J. Atmos. Oceanic Technol.*, **19**, 2030–2048.
- Greco, B., P. Castracane, N. Pierdicca, A. Martini, P. Ciotti, and F. S. Marzano, 2001: A preliminary evaluation of the absolute backscatter calibration of the ERS-1 altimeter using a passive technique. *Proc. IGARSS*, Sydney, Australia, IEEE.
- Jackson, F. C., W. T. Walton, and D. E. Hines, 1992: Sea surface mean square slope from Ku-band backscatter data. *J. Geophys. Res.*, **97**, 11 411–11 427.
- Kozu, T., and Coauthors, 2001: Development of precipitation radar onboard the Tropical Rainfall Measuring Mission (TRMM) satellite. *IEEE Trans. Geosci. Remote Sens.*, **39**, 102–116.
- Kummerow, C., W. Barnes, T. Kozu, J. Shiue, and J. Simpson, 1998: The Tropical Rainfall Measuring Mission (TRMM) sensor package. *J. Atmos. Oceanic Technol.*, **15**, 809–817.
- , and Coauthors, 2000: The status of the Tropical Rainfall Measuring Mission (TRMM) after two years in orbit. *J. Appl. Meteor.*, **39**, 1965–1982.
- Labroue, S., P. Gaspar, J. Dorandeu, O.-Z. Zanife, F. Mertz, P. Vincent, and D. Choquet, 2004: Non-parametric estimates of the sea state bias for Jason-1 radar altimeter. *Mar. Geod.*, **27**, 453–481.
- Lefevre, J., J. Barckicke, and Y. Menard, 1994: A significant wave height dependent function for TOPEX/Poseidon wind speed retrieval. *J. Geophys. Res.*, **99**, 25 035–25 046.
- Leuliette, E. W., R. S. Nerem, and G. T. Mitchum, 2004: Calibration of TOPEX/Poseidon and Jason altimeter data to construct a continuous record of mean sea-level change. *Mar. Geod.*, **27**, 79–94.
- Lin, I.-I., W. Alpers, and W. T. Liu, 2003: First evidence for the detection of natural surface films by the QuikSCAT scatterometer. *Geophys. Res. Lett.*, **30**, 1713, doi:10.1029/2003GL017415.

- Menard, Y., and Coauthors, 2003: The Jason-1 mission. *Mar. Geod.*, **26**, 131–146.
- Millet, F. W., D. V. Arnold, K. F. Warnick, and J. Smith, 2003a: Electromagnetic bias estimation using in situ and satellite data: 1. RMS wave slope. *J. Geophys. Res.*, **108**, 3040, doi:10.1029/2001JC001095.
- , —, —, and —, 2003b: Electromagnetic bias estimation using in situ and satellite data: 2. A nonparametric approach. *J. Geophys. Res.*, **108**, 3041, doi:10.1029/2001JC001144.
- Mitchum, G. T., D. W. Hancock III, G. S. Hayne, and D. Vandemark, 2004: Blooms of σ^0 in the TOPEX radar altimeter data. *J. Atmos. Oceanic Technol.*, **21**, 1232–1245.
- Picot, N., K. Case, S. Desai, and P. Vincent, cited 2003: AVISO and PODAAC user handbook. IGDR and GDR Jason Products, SMM-MU-M5-OP-13184-CN (AVISO), JPL D-21352 (PODAAC). [Available online at www.jason.oceanobs.com/documents/donnees/tool/handbook_jason.pdf.]
- Pierdicca, N., and Coauthors, 2002: Passive calibration of the backscattering coefficient of the Envisat RA-2. *Proc. Int. Geoscience and Remote Sensing Symp.*, Toronto, ON, Canada, IEEE, Vol. 2, 3105–3107.
- Quarty, G. D., 2000: Monitoring and cross-calibration of altimeter σ^0 through dual-frequency backscatter measurements. *J. Atmos. Oceanic Technol.*, **17**, 1252–1258.
- , 2004: Sea state and rain—A second take on dual-frequency altimetry. *Mar. Geod.*, **27**, 133–152.
- Queffeuilou, P., 2003: Long term quality status of wave height and wind speed measurements from satellite altimeters. *Proc. 13th Int. Offshore and Polar Engineering Conf. (ISOPE)*, Honolulu, HI, CD-ROM.
- Quilfen, Y., B. Chapron, F. Collard, and M. Serre, 2004: Calibration/validation of an altimeter wave period model and application to TOPEX/Poseidon and Jason-1 altimeters. *Mar. Geod.*, **27**, 535–549.
- Takahashi, N., H. Kuroiwa, and T. Kawanishi, 2003: Four-year result of external calibration for precipitation radar (PR) of the Tropical Rainfall Measuring Mission (TRMM) satellite. *IEEE Trans. Geosci. Remote Sens.*, **41**, 2398–2403.
- Tournadre, J., 2004: Validation of Jason and Envisat altimeter dual-frequency rain flags. *Mar. Geod.*, **27**, 153–169.
- Tran, N., E. Obligis, and F. Ferreira, 2005: Comparison of two Jason-1 altimeter precipitation detection algorithms with rain estimates from the TRMM Microwave Imager. *J. Atmos. Oceanic Technol.*, **22**, 782–794.
- Vandemark, D., J. B. Edson, and B. Chapron, 1997: Altimeter estimation of sea surface wind stress for light to moderate winds. *J. Atmos. Oceanic Technol.*, **14**, 716–722.
- , B. Chapron, E. J. Walsh, and T. Elfouhaily, 2000: Measurement and modelling of steep ocean wave slopes and absolute calibration of the radar altimeter. *Proc. Int. Geoscience and Remote Sensing Symp. (IGARSS)*, Honolulu, HI, IEEE, Vol. 4, 1495–1497.
- , N. Tran, B. Beckley, B. Chapron, and P. Gaspar, 2002: Direct estimation of sea state impacts on radar altimeter sea level measurements. *Geophys. Res. Lett.*, **29**, 2148, doi:10.1029/2002GL015776.
- Witter, D. L., and D. B. Chelton, 1991: A Geosat altimeter wind speed algorithm and a method for altimeter wind speed algorithm development. *J. Geophys. Res.*, **96**, 8853–8860.